

Observation of a Neutral Charmoniumlike State $Z_c(4025)^0$ in $e^+e^- \rightarrow (D^*\bar{D}^*)^0\pi^0$

M. Ablikim,¹ M. N. Achasov,^{9,f} X. C. Ai,¹ O. Albayrak,⁵ M. Albrecht,⁴ D. J. Ambrose,⁴⁴ A. Amoroso,^{48a,48c} F. F. An,¹ Q. An,^{45,a} J. Z. Bai,¹ R. Baldini Ferroli,^{20a} Y. Ban,³¹ D. W. Bennett,¹⁹ J. V. Bennett,⁵ M. Bertani,^{20a} D. Bettoni,^{21a} J. M. Bian,⁴³ F. Bianchi,^{48a,48c} E. Boger,^{23,d} I. Boyko,²³ R. A. Briere,⁵ H. Cai,⁵⁰ X. Cai,^{1,a} O. Cakir,^{40a,b} A. Calcaterra,^{20a} G. F. Cao,¹ S. A. Cetin,^{40b} J. F. Chang,^{1,a} G. Chelkov,^{23,d,e} G. Chen,¹ H. S. Chen,¹ H. Y. Chen,² J. C. Chen,¹ M. L. Chen,^{1,a} S. J. Chen,²⁹ X. Chen,^{1,a} X. R. Chen,²⁶ Y. B. Chen,^{1,a} H. P. Cheng,¹⁷ X. K. Chu,³¹ G. Cibinetto,^{21a} H. L. Dai,^{1,a} J. P. Dai,³⁴ A. Dbeysy,¹⁴ D. Dedovich,²³ Z. Y. Deng,¹ A. Denig,²² I. Denysenko,²³ M. Destefanis,^{48a,48c} F. De Mori,^{48a,48c} Y. Ding,²⁷ C. Dong,³⁰ J. Dong,^{1,a} L. Y. Dong,¹ M. Y. Dong,^{1,a} S. X. Du,⁵² P. F. Duan,¹ E. E. Eren,^{40b} J. Z. Fan,³⁹ J. Fang,^{1,a} S. S. Fang,¹ X. Fang,^{45,a} Y. Fang,¹ L. Fava,^{48b,48c} F. Feldbauer,²² G. Felici,^{20a} C. Q. Feng,^{45,a} E. Fioravanti,^{21a} M. Fritsch,^{14,22} C. D. Fu,¹ Q. Gao,¹ X. Y. Gao,² Y. Gao,³⁹ Z. Gao,^{45,a} I. Garzia,^{21a} C. Geng,^{45,a} K. Goetzen,¹⁰ W. X. Gong,^{1,a} W. Gradl,²² M. Greco,^{48a,48c} M. H. Gu,^{1,a} Y. T. Gu,¹² Y. H. Guan,¹ A. Q. Guo,¹ L. B. Guo,²⁸ Y. Guo,¹ Y. P. Guo,²² Z. Haddadi,²⁵ A. Hafner,²² S. Han,⁵⁰ Y. L. Han,¹ X. Q. Hao,¹⁵ F. A. Harris,⁴² K. L. He,¹ Z. Y. He,³⁰ T. Held,⁴ Y. K. Heng,^{1,a} Z. L. Hou,¹ C. Hu,²⁸ H. M. Hu,¹ J. F. Hu,^{48a,48c} T. Hu,^{1,a} Y. Hu,¹ G. M. Huang,⁶ G. S. Huang,^{45,a} H. P. Huang,⁵⁰ J. S. Huang,¹⁵ X. T. Huang,³³ Y. Huang,²⁹ T. Hussain,⁴⁷ Q. Ji,¹ Q. P. Ji,³⁰ X. B. Ji,¹ X. L. Ji,^{1,a} L. L. Jiang,¹ L. W. Jiang,⁵⁰ X. S. Jiang,^{1,a} X. Y. Jiang,³⁰ J. B. Jiao,³³ Z. Jiao,¹⁷ D. P. Jin,^{1,a} S. Jin,¹ T. Johansson,⁴⁹ A. Julin,⁴³ N. Kalantar-Nayestanaki,²⁵ X. L. Kang,¹ X. S. Kang,³⁰ M. Kavatsyuk,²⁵ B. C. Ke,⁵ P. Kiese,²² R. Kliemt,¹⁴ B. Kloss,²² O. B. Kolcu,^{40b,i} B. Kopf,⁴ M. Kornicer,⁴² W. Kühn,²⁴ A. Kupsc,⁴⁹ J. S. Lange,²⁴ M. Lara,¹⁹ P. Larin,¹⁴ C. Leng,^{48c} C. Li,⁴⁹ C. H. Li,¹ Cheng Li,^{45,a} D. M. Li,⁵² F. Li,^{1,a} G. Li,¹ H. B. Li,¹ J. C. Li,¹ Jin Li,³² K. Li,¹³ K. Li,³³ Lei Li,³ P. R. Li,⁴¹ T. Li,³³ W. D. Li,¹ W. G. Li,¹ X. L. Li,³³ X. M. Li,¹² X. N. Li,^{1,a} X. Q. Li,³⁰ Z. B. Li,³⁸ H. Liang,^{45,a} Y. F. Liang,³⁶ Y. T. Liang,²⁴ G. R. Liao,¹¹ D. X. Lin,¹⁴ B. J. Liu,¹ C. X. Liu,¹ F. H. Liu,³⁵ Fang Liu,¹ Feng Liu,⁶ H. B. Liu,¹² H. H. Liu,¹⁶ H. H. Liu,¹ H. M. Liu,¹ J. Liu,¹ J. B. Liu,^{45,a} J. P. Liu,⁵⁰ J. Y. Liu,¹ K. Liu,³⁹ K. Y. Liu,²⁷ L. D. Liu,³¹ P. L. Liu,^{1,a} Q. Liu,⁴¹ S. B. Liu,^{45,a} X. Liu,²⁶ X. X. Liu,⁴¹ Y. B. Liu,³⁰ Z. A. Liu,^{1,a} Zhiqiang Liu,¹ Zhiqing Liu,²² H. Loehner,²⁵ X. C. Lou,^{1,a,h} H. J. Lu,¹⁷ J. G. Lu,^{1,a} R. Q. Lu,¹⁸ Y. Lu,¹ Y. P. Lu,^{1,a} C. L. Luo,²⁸ M. X. Luo,⁵¹ T. Luo,⁴² X. L. Luo,^{1,a} M. Lv,¹ X. R. Lyu,⁴¹ F. C. Ma,²⁷ H. L. Ma,¹ L. L. Ma,³³ Q. M. Ma,¹ T. Ma,¹ X. N. Ma,³⁰ X. Y. Ma,^{1,a} F. E. Maas,¹⁴ M. Maggiora,^{48a,48c} Y. J. Mao,³¹ Z. P. Mao,¹ S. Marcello,^{48a,48c} J. G. Messchendorp,²⁵ J. Min,^{1,a} T. J. Min,¹ R. E. Mitchell,¹⁹ X. H. Mo,^{1,a} Y. J. Mo,⁶ C. Morales Morales,¹⁴ K. Moriya,¹⁹ N. Yu. Muchnoi,^{9,f} H. Muramatsu,⁴³ Y. Nefedov,²³ F. Nerling,¹⁴ I. B. Nikolaev,^{9,f} Z. Ning,^{1,a} S. Nisar,⁸ S. L. Niu,^{1,a} X. Y. Niu,¹ S. L. Olsen,³² Q. Ouyang,^{1,a} S. Pacetti,^{20b} P. Patteri,^{20a} M. Pelizaeus,⁴ H. P. Peng,^{45,a} K. Peters,¹⁰ J. Pettersson,⁴⁹ J. L. Ping,²⁸ R. G. Ping,¹ R. Poling,⁴³ V. Prasad,¹ Y. N. Pu,¹⁸ M. Qi,²⁹ S. Qian,^{1,a} C. F. Qiao,⁴¹ L. Q. Qin,³³ N. Qin,⁵⁰ X. S. Qin,¹ Y. Qin,³¹ Z. H. Qin,^{1,a} J. F. Qiu,¹ K. H. Rashid,⁴⁷ C. F. Redmer,²² H. L. Ren,¹⁸ M. Ripka,²² G. Rong,¹ Ch. Rosner,¹⁴ X. D. Ruan,¹² V. Santoro,^{21a} A. Sarantsev,^{23,g} M. Savrié,^{21b} K. Schoenning,⁴⁹ S. Schumann,²² W. Shan,³¹ M. Shao,^{45,a} C. P. Shen,² P. X. Shen,³⁰ X. Y. Shen,¹ H. Y. Sheng,¹ W. M. Song,¹ X. Y. Song,¹ S. Sosio,^{48a,48c} S. Spataro,^{48a,48c} G. X. Sun,¹ J. F. Sun,¹⁵ S. S. Sun,¹ Y. J. Sun,^{45,a} Y. Z. Sun,¹ Z. J. Sun,^{1,a} Z. T. Sun,¹⁹ C. J. Tang,³⁶ X. Tang,¹ I. Tapan,^{40c} E. H. Thorndike,⁴⁴ M. Tiemens,²⁵ M. Ullrich,²⁴ I. Uman,^{40b} G. S. Varner,⁴² B. Wang,³⁰ B. L. Wang,⁴¹ D. Wang,³¹ D. Y. Wang,³¹ K. Wang,^{1,a} L. L. Wang,¹ L. S. Wang,¹ M. Wang,³³ P. Wang,¹ P. L. Wang,¹ S. G. Wang,³¹ W. Wang,^{1,a} X. F. Wang,³⁹ Y. D. Wang,¹⁴ Y. F. Wang,^{1,a} Y. Q. Wang,²² Z. Wang,^{1,a} Z. G. Wang,^{1,a} Z. H. Wang,^{45,a} Z. Y. Wang,¹ T. Weber,²² D. H. Wei,¹¹ J. B. Wei,³¹ P. Weidenkaff,²² S. P. Wen,¹ U. Wiedner,⁴ M. Wolke,⁴⁹ L. H. Wu,¹ Z. Wu,^{1,a} L. G. Xia,³⁹ Y. Xia,¹⁸ D. Xiao,¹ Z. J. Xiao,²⁸ Y. G. Xie,^{1,a} Q. L. Xiu,^{1,a} G. F. Xu,¹ L. Xu,¹ Q. J. Xu,¹³ Q. N. Xu,⁴¹ X. P. Xu,³⁷ L. Yan,^{45,a} W. B. Yan,^{45,a} W. C. Yan,^{45,a} Y. H. Yan,¹⁸ H. J. Yang,³⁴ H. X. Yang,¹ L. Yang,⁵⁰ Y. Yang,⁶ Y. X. Yang,¹¹ H. Ye,¹ M. Ye,^{1,a} M. H. Ye,⁷ J. H. Yin,¹ B. X. Yu,^{1,a} C. X. Yu,³⁰ H. W. Yu,³¹ J. S. Yu,²⁶ C. Z. Yuan,¹ W. L. Yuan,²⁹ Y. Yuan,¹ A. Yuncu,^{40b,c} A. A. Zafar,⁴⁷ A. Zallo,^{20a} Y. Zeng,¹⁸ B. X. Zhang,¹ B. Y. Zhang,^{1,a} C. Zhang,²⁹ C. C. Zhang,¹ D. H. Zhang,¹ H. H. Zhang,³⁸ H. Y. Zhang,^{1,a} J. J. Zhang,¹ J. L. Zhang,¹ J. Q. Zhang,¹ J. W. Zhang,^{1,a} J. Y. Zhang,¹ J. Z. Zhang,¹ K. Zhang,¹ L. Zhang,¹ S. H. Zhang,¹ X. Y. Zhang,³³ Y. Zhang,¹ Y. N. Zhang,⁴¹ Y. H. Zhang,^{1,a} Y. T. Zhang,^{45,a} Yu Zhang,⁴¹ Z. H. Zhang,⁶ Z. P. Zhang,⁴⁵ Z. Y. Zhang,⁵⁰ G. Zhao,¹ J. W. Zhao,^{1,a} J. Y. Zhao,¹ J. Z. Zhao,^{1,a} Lei Zhao,^{45,a} Ling Zhao,¹ M. G. Zhao,³⁰ Q. Zhao,¹ Q. W. Zhao,¹ S. J. Zhao,⁵² T. C. Zhao,¹ Y. B. Zhao,^{1,a} Z. G. Zhao,^{45,a} A. Zhemchugov,^{23,d} B. Zheng,⁴⁶ J. P. Zheng,^{1,a} W. J. Zheng,³³ Y. H. Zheng,⁴¹ B. Zhong,²⁸ L. Zhou,^{1,a} Li Zhou,³⁰ X. Zhou,⁵⁰ X. K. Zhou,^{45,a} X. R. Zhou,^{45,a} X. Y. Zhou,¹ K. Zhu,¹ K. J. Zhu,^{1,a} S. Zhu,¹ X. L. Zhu,³⁹ Y. C. Zhu,^{45,a} Y. S. Zhu,¹ Z. A. Zhu,¹ J. Zhuang,^{1,a} L. Zotti,^{48a,48c} B. S. Zou,¹ and J. H. Zou¹

(BESIII Collaboration)

- ¹*Institute of High Energy Physics, Beijing 100049, People's Republic of China*
²*Beihang University, Beijing 100191, People's Republic of China*
³*Beijing Institute of Petrochemical Technology, Beijing 102617, People's Republic of China*
⁴*Bochum Ruhr-University, D-44780 Bochum, Germany*
⁵*Carnegie Mellon University, Pittsburgh, Pennsylvania 15213, USA*
⁶*Central China Normal University, Wuhan 430079, People's Republic of China*
⁷*China Center of Advanced Science and Technology, Beijing 100190, People's Republic of China*
⁸*COMSATS Institute of Information Technology, Lahore, Defence Road, Off Raiwind Road, 54000 Lahore, Pakistan*
⁹*G.I. Budker Institute of Nuclear Physics SB RAS (BINP), Novosibirsk 630090, Russia*
¹⁰*GSI Helmholtzcentre for Heavy Ion Research GmbH, D-64291 Darmstadt, Germany*
¹¹*Guangxi Normal University, Guilin 541004, People's Republic of China*
¹²*GuangXi University, Nanning 530004, People's Republic of China*
¹³*Hangzhou Normal University, Hangzhou 310036, People's Republic of China*
¹⁴*Helmholtz Institute Mainz, Johann-Joachim-Becher-Weg 45, D-55099 Mainz, Germany*
¹⁵*Henan Normal University, Xinxiang 453007, People's Republic of China*
¹⁶*Henan University of Science and Technology, Luoyang 471003, People's Republic of China*
¹⁷*Huangshan College, Huangshan 245000, People's Republic of China*
¹⁸*Hunan University, Changsha 410082, People's Republic of China*
¹⁹*Indiana University, Bloomington, Indiana 47405, USA*
^{20a}*INFN Laboratori Nazionali di Frascati, I-00044 Frascati, Italy*
^{20b}*INFN and University of Perugia, I-06100 Perugia, Italy*
^{21a}*INFN Sezione di Ferrara, I-44122 Ferrara, Italy*
^{21b}*University of Ferrara, I-44122 Ferrara, Italy*
²²*Johannes Gutenberg University of Mainz, Johann-Joachim-Becher-Weg 45, D-55099 Mainz, Germany*
²³*Joint Institute for Nuclear Research, 141980 Dubna, Moscow Region, Russia*
²⁴*Justus Liebig University Giessen, II. Physikalisches Institut, Heinrich-Buff-Ring 16, D-35392 Giessen, Germany*
²⁵*KVI-CART, University of Groningen, NL-9747 AA Groningen, Netherlands*
²⁶*Lanzhou University, Lanzhou 730000, People's Republic of China*
²⁷*Liaoning University, Shenyang 110036, People's Republic of China*
²⁸*Nanjing Normal University, Nanjing 210023, People's Republic of China*
²⁹*Nanjing University, Nanjing 210093, People's Republic of China*
³⁰*Nankai University, Tianjin 300071, People's Republic of China*
³¹*Peking University, Beijing 100871, People's Republic of China*
³²*Seoul National University, Seoul 151-747, Korea*
³³*Shandong University, Jinan 250100, People's Republic of China*
³⁴*Shanghai Jiao Tong University, Shanghai 200240, People's Republic of China*
³⁵*Shanxi University, Taiyuan 030006, People's Republic of China*
³⁶*Sichuan University, Chengdu 610064, People's Republic of China*
³⁷*Soochow University, Suzhou 215006, People's Republic of China*
³⁸*Sun Yat-Sen University, Guangzhou 510275, People's Republic of China*
³⁹*Tsinghua University, Beijing 100084, People's Republic of China*
^{40a}*Istanbul Aydin University, 34295 Sefakoy, Istanbul, Turkey*
^{40b}*Dogus University, 34722 Istanbul, Turkey*
^{40c}*Uludag University, 16059 Bursa, Turkey*
⁴¹*University of Chinese Academy of Sciences, Beijing 100049, People's Republic of China*
⁴²*University of Hawaii, Honolulu, Hawaii 96822, USA*
⁴³*University of Minnesota, Minneapolis, Minnesota 55455, USA*
⁴⁴*University of Rochester, Rochester, New York 14627, USA*
⁴⁵*University of Science and Technology of China, Hefei 230026, People's Republic of China*
⁴⁶*University of South China, Hengyang 421001, People's Republic of China*
⁴⁷*University of the Punjab, Lahore 54590, Pakistan*
^{48a}*University of Turin, I-10125 Turin, Italy*
^{48b}*University of Eastern Piedmont, I-15121 Alessandria, Italy*
^{48c}*INFN, I-10125 Turin, Italy*
⁴⁹*Uppsala University, Box 516, SE-75120 Uppsala, Sweden*
⁵⁰*Wuhan University, Wuhan 430072, People's Republic of China*
⁵¹*Zhejiang University, Hangzhou 310027, People's Republic of China*
⁵²*Zhengzhou University, Zhengzhou 450001, People's Republic of China*

(Received 9 July 2015; revised manuscript received 19 September 2015; published 29 October 2015)

We report a study of the process $e^+e^- \rightarrow (D^*\bar{D}^*)^0\pi^0$ using e^+e^- collision data samples with integrated luminosities of 1092 pb^{-1} at $\sqrt{s} = 4.23 \text{ GeV}$ and 826 pb^{-1} at $\sqrt{s} = 4.26 \text{ GeV}$ collected with the BESIII detector at the BEPCII storage ring. We observe a new neutral structure near the $(D^*\bar{D}^*)^0$ mass threshold in the π^0 recoil mass spectrum, which we denote as $Z_c(4025)^0$. Assuming a Breit-Wigner line shape, its pole mass and pole width are determined to be $(4025.5_{-4.7}^{+2.0} \pm 3.1) \text{ MeV}/c^2$ and $(23.0 \pm 6.0 \pm 1.0) \text{ MeV}$, respectively. The Born cross sections of $e^+e^- \rightarrow Z_c(4025)^0\pi^0 \rightarrow (D^*\bar{D}^*)^0\pi^0$ are measured to be $(61.6 \pm 8.2 \pm 9.0) \text{ pb}$ at $\sqrt{s} = 4.23 \text{ GeV}$ and $(43.4 \pm 8.0 \pm 5.4) \text{ pb}$ at $\sqrt{s} = 4.26 \text{ GeV}$. The first uncertainties are statistical and the second are systematic.

DOI: 10.1103/PhysRevLett.115.182002

PACS numbers: 14.40.Rt, 13.25.Gv, 13.66.Bc

Recent discoveries of new charmoniumlike states that do not fit naturally with the predictions of the quark model have generated great experimental and theoretical interest [1]. Among these so-called XYZ particles are charged states with decay modes that clearly demonstrate a structure consisting of at least four quarks, including a $c\bar{c}$ pair. The first charged charmoniumlike state $Z(4430)^+$ was discovered by Belle [2]. LHCb confirmed the existence of this state. Belle determined its spin-parity to be 1^+ [3], which is supported by a new result from LHCb [4]. Recently, the BESIII Collaboration observed four charged Z_c states, $Z_c(3885)^\pm$ [5], $Z_c(3900)^\pm$ [6], $Z_c(4020)^\pm$ [7], and $Z_c(4025)^\pm$ [8], produced in $e^+e^- \rightarrow \pi^\mp Z_c^\pm$. The observed decay channels are $Z_c(3900)^\pm \rightarrow \pi^\mp J/\psi$, $Z_c(3885)^\pm \rightarrow (D\bar{D}^*)^\pm$, $Z_c(4020)^\pm \rightarrow \pi^\pm h_c$, and $Z_c(4025)^\pm \rightarrow (D^*\bar{D}^*)^\pm$. These states are close to the $D\bar{D}^*$ or $D^*\bar{D}^*$ threshold. The $Z_c(3900)^\pm$ was also observed by Belle [9] and with CLEO-c data [10].

Thus far, the nature of these new states has been elusive. Interpretations in terms of tetraquarks, molecules, hadro-charmonium, and cusp effects have been proposed [11–19]. Searching for their neutral partners in experiments is of great importance in understanding their properties, especially for identifying their isospin properties. Previously, based on CLEO-c data, evidence of a neutral state $Z_c(3900)^0$ decaying to $\pi^0 J/\psi$ [20] was reported. Recently, two neutral states, $Z_c(3900)^0$ and $Z_c(4020)^0$, were discovered in their decays, $Z_c(3900)^0 \rightarrow \pi^0 J/\psi$ and $Z_c(4020)^0 \rightarrow \pi^0 h_c$, by BESIII [21,22]. These can be interpreted as the isospin partners of the $Z_c(3900)^\pm$ and $Z_c(4020)^\pm$. Analogously, it is natural to search for the neutral partner of the $Z_c(4025)^\pm$ [8] in its decay to $(D^*\bar{D}^*)^0$.

In this Letter, we report a search for the neutral partner of the $Z_c(4025)^\pm$ through the reactions $e^+e^- \rightarrow D^{*0}\bar{D}^{*0}(D^{*+}D^{*-})\pi^0$, as the charged $Z_c(4025)^\pm$ [8] couples to $(D^*\bar{D}^*)^\pm$ and has a mass close to the $(D^*\bar{D}^*)^\pm$ mass threshold. We denote the investigated final state products as $(D^*\bar{D}^*)^0\pi^0$, where D^* refers to D^{*0} or D^{*+} and \bar{D}^* stands for their antiparticles. A partial reconstruction method is applied to identify the $(D^*\bar{D}^*)^0\pi^0$ final states. This method requires detection of a D and a \bar{D} originating from D^* and \bar{D}^* decays of $D^* \rightarrow D\pi$ and $D\gamma$, and the π^0 from the primary production (denoted as the *bachelor* π^0). The data sample analyzed

corresponds to e^+e^- collisions with integrated luminosities of 1092 pb^{-1} at $\sqrt{s} = 4.23 \text{ GeV}$ and 826 pb^{-1} at $\sqrt{s} = 4.26 \text{ GeV}$ [23] collected with the BESIII detector [24] at the BEPCII storage ring [25].

BESIII is a cylindrically symmetric detector which, from inner to outer parts, consists of the following components: a helium-gas based multilayer drift chamber (MDC), a time-of-flight counter (TOF), a CsI(Tl) crystal electromagnetic calorimeter (EMC), a 1-T superconducting solenoid magnet and a nine-layer resistive-plate-chamber-based muon chamber system. The momentum resolution for charged tracks in the MDC is 0.5% at a momentum of $1 \text{ GeV}/c$. The energy resolution for photons in EMC with an energy of 1 GeV is 2.5% for the center region (the barrel) and 5% for the rest of the detector (the end caps). For charged particle identification (PID), probabilities $\mathcal{L}(h)$ for particle hypotheses $h = \pi$ or K are evaluated based on the normalized energy loss dE/dx in the MDC and the time of flight in the TOF. More details on the BESIII spectrometer can be found in Ref. [24].

To optimize data-selection criteria, understand backgrounds, and estimate the detection efficiency, we simulate the e^+e^- annihilation processes with the KKMC algorithm [26], which takes into account continuum processes, initial state radiation (ISR) return to ψ and Y states, and inclusive $D_{(s)}$ production. The known decay rates are taken from the Particle Data Group (PDG) [27] and the decays are modeled with EVTGEN [28]. The remaining decays are simulated with the LUNDCHARM package [29]. The nonresonant, three-body phase space (PHSP) processes $e^+e^- \rightarrow D^*\bar{D}^*\pi^0$ are simulated according to uniform distributions in momentum phase space. We assume that $Z_c(4025)^0$ has a spin-parity of 1^+ by considering the measurements of other Z resonances [3,4] and the signal process $e^+e^- \rightarrow Z_c(4025)^0\pi^0$ followed by $Z_c(4025)^0 \rightarrow (D^*\bar{D}^*)^0$ proceeds in S waves. The D^* is required to decay inclusively according to its decay branching ratios from PDG [27]. The D^+ is required to decay into $K^-\pi^+\pi^+$, while D^0 is required to decay into $K^-\pi^+$, $K^-\pi^+\pi^0$, and $K^-\pi^+\pi^+\pi^-$. These decay modes are the ones used to reconstruct D mesons [30]. All simulated MC events are fed into a GEANT4-based [31] software package, taking into account detector geometry and response.

The charged tracks of K^- and π^\pm are reconstructed in the MDC. For each charged track, the polar angle θ defined with respect to the e^+ beam is required to satisfy $|\cos\theta| < 0.93$. The closest approach to the e^+e^- interaction point is required to be within ± 10 cm along the beam direction and within 1 cm in the plane perpendicular to the beam direction. A track is identified to be a $K(\pi)$ when the PID probabilities satisfy $\mathcal{L}(K) > \mathcal{L}(\pi)$ [$\mathcal{L}(K) < \mathcal{L}(\pi)$], according to the information from dE/dx and the TOF.

The π^0 candidates are reconstructed by combining pairs of photons reconstructed in the EMC that are not associated with charged tracks. For each photon, the energy deposition in the EMC barrel region is required to be greater than 25 MeV, while in the end-cap region, it must be greater than 50 MeV due to the differing detector resolution and the probability of reconstructing a fake photon. To suppress electronics noise and energy deposits unrelated to the event, the EMC cluster time is restricted to be within a 700 ns window near the event start time. The invariant mass of any pair of photons $M(\gamma\gamma)$ is required to be within (0.120, 0.145) GeV/c^2 and is constrained to the nominal π^0 mass. The kinematics of the two photons is updated according to the constraint fit.

We consider all possible combinations of selected charged tracks and π^0 to form D candidates. The charged tracks from a D decay candidate are required to originate from a common vertex. The χ^2_{VF} of the vertex fit is required to satisfy $\chi^2_{\text{VF}} < 100$. We constrain the reconstructed masses of the final state particles to the corresponding D nominal masses and require $\chi^2_{\text{KF}}(D)$ for the kinematic fit to be less than 15 for the final states of D decays including charged tracks only, and less than 20 for the final state including π^0 . We select signal event candidates which consist of at least one pair of $D\bar{D}$ candidates that do not share particles in the final state. If there is more than one pair of $D\bar{D}$ candidates in an event, only the one with the minimum $\chi^2_{\text{KF}}(D) + \chi^2_{\text{KF}}(\bar{D})$ is kept for further analysis.

We reconstruct the bachelor π^0 from the remaining photon showers that are not assigned to the $D\bar{D}$ pair. To further reject backgrounds, each photon candidate originating from the bachelor π^0 is required not to form a π^0 candidate with any other photon in the event. A mass constraint of the two photons to the π^0 nominal mass is implemented and the corresponding fit quality is required to satisfy $\chi^2_{\text{KF}}(\pi^0) < 20$. To reject the background for the bachelor π^0 from $D^* \rightarrow D\pi^0$ decays, we require the $D\pi^0$ invariant mass to be greater than 2.02 GeV/c^2 .

To identify the decay products of the signal process $e^+e^- \rightarrow D^*\bar{D}^*\pi^0$, we plot the recoil mass spectra of $D\pi^0$ [$\text{RM}(D\pi^0)$], as shown in Fig. 1. The peaks around 2 GeV/c^2 correspond to the process $e^+e^- \rightarrow D\bar{D}^*\pi^0$ with a missing \bar{D}^* . Besides these peaks, we see clear bumps around 2.15 GeV/c^2 in the data. These bumps are

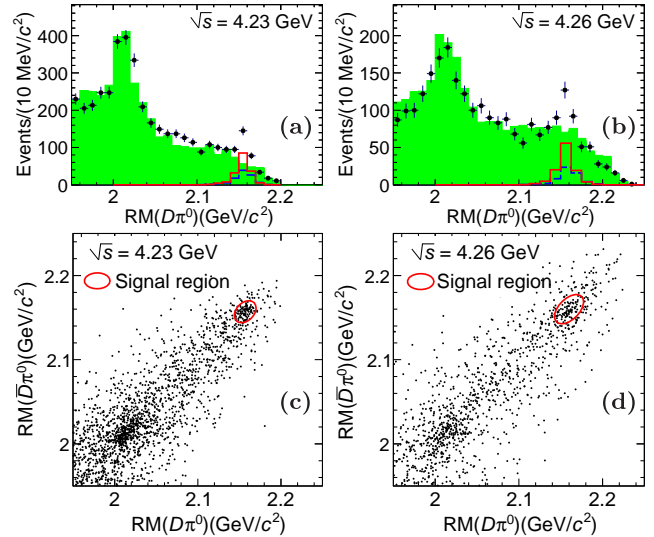


FIG. 1 (color online). Distributions of $\text{RM}(D\pi^0)$ at $\sqrt{s} = 4.23$ GeV (a) and $\sqrt{s} = 4.26$ GeV (b). Points with error bars are data and the shaded histograms represent the inclusive backgrounds in MC simulations. The solid line and the dashed line are the $Z_c(4025)^0$ signal shape and the PHSP shape with arbitrary normalization, respectively. The third row gives the scatter plot of $\text{RM}(D\pi^0)$ vs $\text{RM}(\bar{D}\pi^0)$ at $\sqrt{s} = 4.23$ GeV (c) and $\sqrt{s} = 4.26$ GeV (d), where the solid ovals indicate the signal regions.

consistent with the MC simulations of the $D^*\bar{D}^*\pi^0$ final state. The peak position roughly corresponds to the sum of the mass of D^* and the mass of a π , since the π originating from D^* is soft and is not used in the computation of the recoil mass. The backgrounds beneath the bumps are mostly from ISR production of the $D^*\bar{D}^*$ process. Other processes, such as $e^+e^- \rightarrow D^*\bar{D}^{**} \rightarrow D^*\bar{D}^*\pi^0$, are expected to be absent, according to simulation studies. This is understandable because the process $D_0^*(2400) \rightarrow D^*\pi^0$ is forbidden due to the conservation of spin-parity. $D_1^*(2420)^0$ [$D_2^*(2460)^0$] is narrow, and the sum of the mass of $D_1^*(2420)^0$ [$D_2^*(2460)^0$] and D^* is much larger than 4.26 GeV. To extract the signals, we keep events within the two-dimensional oval regions in the distributions of $\text{RM}(D\pi^0)$ and $\text{RM}(\bar{D}\pi^0)$ shown in Figs. 1(c) and 1(d). We choose the specific dimensions due to different resolutions at different momentum phase spaces at two energy points. They are determined according to MC simulation.

The selected events are used to produce the recoil mass distribution of the bachelor π^0 [$\text{RM}(\pi^0)$], shown in Fig. 2. We observe enhancements in the $\text{RM}(\pi^0)$ distribution over the inclusive backgrounds for both data samples, which can not be explained by three-body nonresonant processes. We assume the presence of an S -wave Breit-Wigner resonance structure [denoted as $Z_c(4025)^0$] with a mass-dependent width, using the form given in Ref. [32]:

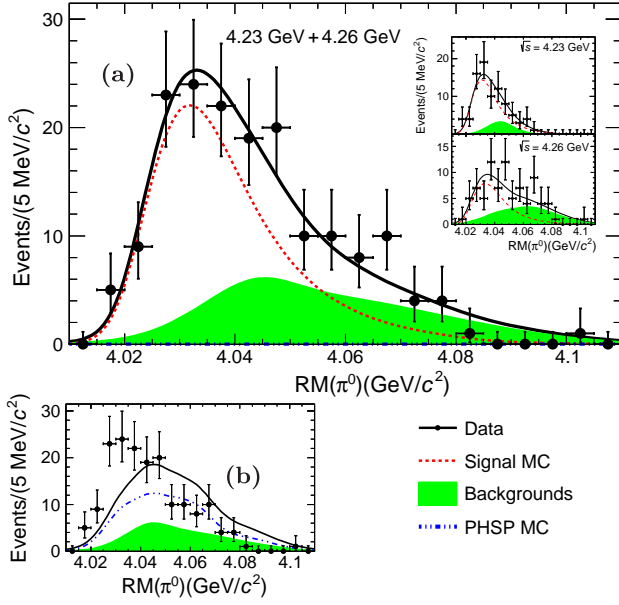


FIG. 2 (color online). Fits to $RM(\pi^0)$. (a) A fit to the background, PHSP, and $Z_c(4025)^0$ signal process for the combination of all data (main panel), and the two collision energies separately (insets). (b) Fits using only the inclusive background and PHSP. The points with error bars are the data, the solid line is the sum of fit functions, the dotted line stands for the $Z_c(4025)^0$ signals, the filled area represents the inclusive backgrounds, and the dash-dotted line is the PHSP process.

$$\left| \frac{1}{M^2 - m^2 - im[\Gamma_1(M) + \Gamma_2(M)]/c^2} \right|^2 p_k q_k,$$

and $\Gamma_k(M) = f_k \Gamma \frac{p_k m}{p_k^* M} (k = 1, 2).$

Here, $k = 1$ and 2 denote the neutral channel $Z_c(4025)^0 \rightarrow D^{*0} \bar{D}^{*0}$ and the charged channel $Z_c(4025)^0 \rightarrow D^{*+} D^{*-}$, respectively. f_k is the ratio of the partial decay width for channel k . M is the reconstructed mass, m is the resonance mass, and Γ is the resonance width. $p_k(q_k)$ is the $D^*(\pi^0)$ momentum in the rest frame of the $D^* \bar{D}^*$ system (the initial $e^+ e^-$ system) and p_k^* is the momentum of D^* in the $Z_c(4025)^0$ rest frame at $M = m$. We assume that the $Z_c(4025)^0$ decay rates to the neutral channel and the charged channel are equal, i.e., $f_k = 0.5$, based on isospin symmetry.

We perform a simultaneous unbinned maximum likelihood fit to the spectra of $RM(\pi^0)$ at $\sqrt{s} = 4.23$ and 4.26 GeV. The signal shapes are taken as convolutions of the efficiency-weighted Breit-Wigner functions with resolution functions obtained from MC simulations. The detector resolutions are 4 MeV at $\sqrt{s} = 4.23$ GeV and 4.5 MeV at $\sqrt{s} = 4.26$ GeV. Backgrounds are modeled with kernel-estimated nonparametric shapes [33] based on the inclusive MC simulations, and their magnitudes are fixed according to the simulations since the inclusive MC samples well describe the background. The shape of

the PHSP process is adopted from MC simulations. We combine the data at $\sqrt{s} = 4.23$ GeV and $\sqrt{s} = 4.26$ GeV together, as shown in Fig. 2. The fit determines m and Γ to be (4031.7 ± 2.1) MeV/ c^2 and (25.9 ± 8.8) MeV, respectively. The corresponding pole position $m_{\text{pole}}(Z_c(4025)^0) - i[\Gamma_{\text{pole}}(Z_c(4025)^0)/2]$ is calculated to be

$$m_{\text{pole}}(Z_c(4025)^0) = (4025.5_{-4.7}^{+2.0}) \text{ MeV}/c^2,$$

$$\Gamma_{\text{pole}}(Z_c(4025)^0) = (23.0 \pm 6.0) \text{ MeV}.$$

The significance with systematic errors is estimated by comparing the likelihoods of the fits with and without the $Z_c(4025)^0$ signal component included. The likelihood difference is $2\Delta \ln L = 45.3$ and the difference of the number of free parameters is 4 . When the systematic uncertainties are taken into account with the assumption of Gaussian distribution, the significance is estimated to be 5.9σ .

The Born cross section $\sigma(e^+ e^- \rightarrow Z_c(4025)^0 \pi^0 \rightarrow (D^{*0} \bar{D}^{*0} + D^{*+} D^{*-}) \pi^0)$ is calculated from the equation

$$\sigma = \frac{n_{\text{sig}}}{\mathcal{L}(f_1 \mathcal{B}_1 \varepsilon_1 + f_2 \mathcal{B}_2 \varepsilon_2)(1 + \delta)(1 + \delta_{\text{vac}})},$$

where \mathcal{L} is the integrated luminosity, ε_1 (ε_2) is the detection efficiency of the neutral (charged) channel, f_1 (f_2) is the ratio of the cross section of the neutral (charged) channel to the sum of both channels, \mathcal{B}_1 (\mathcal{B}_2) is the product branching fraction of the neutral (charged) D^* decays to the final states we detected. $(1 + \delta)$ is the radiative correction factor and $(1 + \delta_{\text{vac}})$ is the vacuum polarization factor. From the simultaneous fit, we obtain 69.5 ± 9.2 signal events at $\sqrt{s} = 4.23$ GeV and 46.1 ± 8.5 signal events at $\sqrt{s} = 4.26$ GeV. $(1 + \delta)$ is calculated to be 0.744 at $\sqrt{s} = 4.23$ GeV and 0.793 at $\sqrt{s} = 4.26$ GeV to the second order in QED [34], where the input line shape of the cross section is assumed to be the same as for $e^+ e^- \rightarrow (D^* \bar{D}^*)^+ \pi^-$, as extracted directly from BESIII data. $(1 + \delta_{\text{vac}})$ is given as 1.054 following the formula in Ref. [35]. The efficiency ε_1 (ε_2) is determined to be 1.49% (3.87%) at $\sqrt{s} = 4.23$ GeV and 1.84% (4.37%) at $\sqrt{s} = 4.26$ GeV. Thus, the cross sections are measured to be (61.6 ± 8.2) pb and (43.4 ± 8.0) pb at $\sqrt{s} = 4.23$ and 4.26 GeV, respectively. The contribution of the PHSP process is found to be negligible according to the fit.

Sources of systematic uncertainties in the measurement of the $Z_c(4025)^0$ resonance parameters and cross sections are listed in Table I. Uncertainties of tracking and PID are each 1% per track [36]. The uncertainty of the π^0 reconstruction efficiency is 4% [37]. We study the photon veto by fitting the recoil mass of $D\pi^0$ with and without this veto in selecting the control sample of $e^+ e^- \rightarrow (D^* \bar{D}^*)^0 \pi^0$ in the data. The efficiency-corrected signal yields are used

TABLE I. Summary of systematic uncertainties on the $Z_c(4025)^0$ resonance parameters and cross sections σ_{4230} at $\sqrt{s} = 4.23$ GeV and σ_{4260} at 4.26 GeV. “...” means that the uncertainty is negligible. The total systematic uncertainty is taken as the root of the quadratic sum of the individual uncertainties.

Source	$m(\text{MeV}/c^2)$	$\Gamma(\text{MeV})$	$\sigma_{4230}(\%)$	$\sigma_{4260}(\%)$
Tracking			5	5
Particle ID			5	5
π^0 reconstruction			4	4
Photon veto			4.2	4.2
Mass scale	2.6			
Detector resolution	0.2	0.1	0.3	0.5
Backgrounds	0.6	0.2	5.6	5.4
Oval cut	1.5	1.0	4.2	2.0
Fit range	...	0.1	0.3	0.5
$D^*\bar{D}^*\pi^0$ line shape	6.0	3.0
Luminosity			1	1
\mathcal{B}_1 and \mathcal{B}_2	6.5	5.3
Isospin violation	...	0.2	0.3	0.2
Vacuum polarization			0.5	0.5
Total	3.1	1.0	14.6	12.5

to extract the cross section, and the corresponding change is taken into account as the systematic error introduced by this requirement. The systematic uncertainties are determined to be 4.2% for both data samples. The mass-scale uncertainty for the $Z_c(4025)^0$ mass is estimated with the mass shift (a comparison between the PDG nominal values and the fit values) of $\text{RM}(D\pi^0)$ in the control sample $e^+e^- \rightarrow D\bar{D}\pi^0$ and of $\text{RM}(D)$ in the control sample of $e^+e^- \rightarrow D\bar{D}$. To be conservative, the largest difference of the two mass shifts, 2.6 MeV/ c^2 , is assigned as the systematic uncertainty due to the mass scale. The systematic uncertainty from the backgrounds is estimated by leaving free the magnitudes in the fit and making different choices in nonparametric kernel estimation of the background events to account for the limited precision in the MC simulation [38]. We change the oval cut criteria and take the largest difference as the systematic uncertainty. Since the line shape will affect the efficiency and $(1 + \delta)$, to evaluate the systematic uncertainties with respect to the input $D^*\bar{D}^*\pi^0$ line shape, we change its shape based on uncertainties of the observed $D^{*+}\bar{D}^{*0}\pi^-$ cross section. Branching fractions \mathcal{B}_1 and \mathcal{B}_2 are used in calculating the cross sections, and the uncertainties of the world average results are included as part of the systematic uncertainty.

Other items in Table I have only minor effects on the precision of the results. We change the fitting ranges in the $\text{RM}(\pi^0)$ spectrum and take the largest difference as the systematic uncertainty. The uncertainties due to detector resolution are accounted for by varying the widths of the smearing functions. The uncertainty of integrated luminosity is determined to be 1% by measuring large angle

Bhabha events [7]. We vary the ratio f_k from 0.4 to 0.6 to take into account potential isospin violation between the neutral and charged processes. The corresponding changes are assigned as systematic uncertainties. The systematic uncertainty of the vacuum polarization factor is 0.5% [35].

In summary, using e^+e^- annihilation data at $\sqrt{s} = 4.23$ and 4.26 GeV, we observe enhancements in the π^0 recoil mass spectrum in the process $e^+e^- \rightarrow D^{*0}\bar{D}^{*0}(D^{*+}D^{*-})\pi^0$. Assuming that the enhancement is due to a neutral charmoniumlike state decaying to $D^*\bar{D}^*$ and that it has a spin-parity of 1^+ , the mass and the width of its pole position are determined to be $m_{\text{pole}}(Z_c(4025)^0) = (4025.5_{-4.7}^{+2.0} \pm 3.1)$ MeV/ c^2 and $\Gamma_{\text{pole}}(Z_c(4025)^0) = (23.0 \pm 6.0 \pm 1.0)$ MeV, respectively. The Born cross section $\sigma(e^+e^- \rightarrow Z_c(4025)^0\pi^0 \rightarrow (D^{*0}\bar{D}^{*0} + D^{*+}D^{*-})\pi^0)$ is measured to be $(61.6 \pm 8.2 \pm 9.0)$ pb at $\sqrt{s} = 4.23$ GeV and $(43.4 \pm 8.0 \pm 5.4)$ pb at $\sqrt{s} = 4.26$ GeV. Hence, we estimate the ratio $[\sigma(e^+e^- \rightarrow Z_c(4025)^0\pi^0 \rightarrow (D^*\bar{D}^*)^0\pi^0)/\sigma(e^+e^- \rightarrow Z_c(4025)^+\pi^- \rightarrow (D^*\bar{D}^*)^+\pi^-)]$ to be compatible with unity at $\sqrt{s} = 4.26$ GeV, which is expected from isospin symmetry. In addition, the $Z_c(4025)^0$ has mass and width very close to those of the $Z_c(4025)^\pm$, which couples to $(D^*\bar{D}^*)^\pm$ [8]. Therefore, the observed $Z_c(4025)^0$ state in this Letter is a good candidate to be the isospin partner of $Z_c(4025)^\pm$.

The BESIII Collaboration thanks the staff of BEPCII and the IHEP computing center for their strong support. This work is supported in part by the National Key Basic Research Program of China under Contract No. 2015CB856700; the National Natural Science Foundation of China (NSFC) under Contracts No. 11125525, No. 11235011, No. 11275266, No. 11322544, No. 11335008, and No. 11425524; the Chinese Academy of Sciences (CAS) Large-Scale Scientific Facility Program; the CAS Center for Excellence in Particle Physics (CCEPP); the Collaborative Innovation Center for Particles and Interactions (CICPI); the Joint Large-Scale Scientific Facility Funds of the NSFC and the CAS under Contracts No. 11179007, No. U1232201, and No. U1332201; the CAS under Contracts No. KJCX2-YW-N29 and No. KJCX2-YW-N45; the 100 Talents Program of the CAS; INPAC and the Shanghai Key Laboratory for Particle Physics and Cosmology; German Research Foundation DFG under Contract No. Collaborative Research Center CRC-1044; the Istituto Nazionale di Fisica Nucleare, Italy; the Ministry of Development of Turkey under Contract No. DPT2006K-120470; the Russian Foundation for Basic Research under Contract No. 14-07-91152; the U.S. Department of Energy under Contracts No. DE-FG02-04ER41291, No. E-FG02-05ER41374, No. DE-FG02-94ER40823, and No. DESC0010118; the U.S. National Science Foundation; the University of Groningen (RuG) and the Helmholtzzentrum fuer Schwerionenforschung GmbH (GSI), Darmstadt; and the WCU Program of National Research Foundation of Korea under Contract No. R32-2008-000-10155-0.

- ^aAlso at State Key Laboratory of Particle Detection and Electronics, Beijing 100049, Hefei 230026, People's Republic of China.
- ^bAlso at Ankara University, 06100 Tandogan, Ankara, Turkey.
- ^cAlso at Bogazici University, 34342 Istanbul, Turkey.
- ^dAlso at the Moscow Institute of Physics and Technology, Moscow 141700, Russia.
- ^eAlso at the Functional Electronics Laboratory, Tomsk State University, Tomsk 634050, Russia.
- ^fAlso at the Novosibirsk State University, Novosibirsk 630090, Russia.
- ^gAlso at the NRC "Kurchatov" Institute, PNPI, 188300 Gatchina, Russia.
- ^hAlso at University of Texas at Dallas, Richardson, Texas 75083, USA.
- ⁱPresent address: Istanbul Arel University, 34295 Istanbul, Turkey.
- [1] G. T. Bodwin, E. Braaten, E. Eichten, S. L. Olsen, T. K. Pedlar, and J. Russ, *arXiv:1307.7425*; X. Liu, *Chin. Sci. Bull.* **59**, 3815 (2014); S. L. Olsen, *Front. Phys.* **10**, 101401 (2015).
- [2] S. K. Choi *et al.* (Belle Collaboration), *Phys. Rev. Lett.* **100**, 142001 (2008).
- [3] K. Chilikin *et al.* (Belle Collaboration), *Phys. Rev. D* **88**, 074026 (2013).
- [4] R. Aaij *et al.* (LHCb Collaboration), *Phys. Rev. Lett.* **112**, 222002 (2014).
- [5] M. Ablikim *et al.* (BESIII Collaboration), *Phys. Rev. Lett.* **112**, 022001 (2014).
- [6] M. Ablikim *et al.* (BESIII Collaboration), *Phys. Rev. Lett.* **110**, 252001 (2013).
- [7] M. Ablikim *et al.* (BESIII Collaboration), *Phys. Rev. Lett.* **111**, 242001 (2013).
- [8] M. Ablikim *et al.* (BESIII Collaboration), *Phys. Rev. Lett.* **112**, 132001 (2014).
- [9] Z. Q. Liu *et al.* (Belle Collaboration), *Phys. Rev. Lett.* **110**, 252002 (2013).
- [10] T. Xiao, S. Dobbs, A. Tomaradze, and K. K. Seth, *Phys. Lett. B* **727**, 366 (2013).
- [11] D. Y. Chen, X. Liu, and T. Matsuki, *Phys. Rev. D* **88**, 036008 (2013).
- [12] Z. F. Sun, J. He, X. Liu, Z. G. Luo, and S. L. Zhu, *Phys. Rev. D* **84**, 054002 (2011).
- [13] Z. F. Sun, Z. G. Luo, J. He, X. Liu, and S. L. Zhu, *Chin. Phys. C* **36**, 194 (2012).
- [14] Q. Wang, C. Hanhart, and Q. Zhao, *Phys. Rev. Lett.* **111**, 132003 (2013).
- [15] F. K. Guo, C. Hidalgo-Duque, J. Nieves, and M. Pavon Valderrama, *Phys. Rev. D* **88**, 054007 (2013).
- [16] J. R. Zhang, *Phys. Rev. D* **87**, 116004 (2013).
- [17] Q. Y. Lin, X. Liu, and H. S. Xu, *Phys. Rev. D* **88**, 114009 (2013).
- [18] X. Wang, Y. Sun, D. Y. Chen, X. Liu, and T. Matsuki, *Eur. Phys. J. C* **74**, 2761 (2014).
- [19] A. Martinez Torres, K. P. Khemchandani, F. S. Navarra, M. Nielsen, and E. Oset, *Phys. Rev. D* **89**, 014025 (2014).
- [20] T. Xiao, S. Dobbs, A. Tomaradze, and K. K. Seth, *Phys. Lett. B* **727**, 366 (2013).
- [21] M. Ablikim *et al.* (BESIII Collaboration), *Phys. Rev. Lett.* **115**, 112003 (2015).
- [22] M. Ablikim *et al.* (BESIII Collaboration), *Phys. Rev. Lett.* **113**, 212002 (2014).
- [23] M. Ablikim *et al.* (BESIII Collaboration), *Chin. Phys. C* **39**, 093001 (2015).
- [24] M. Ablikim *et al.* (BESIII Collaboration), *Nucl. Instrum. Methods Phys. Res., Sect. A* **614**, 345 (2010).
- [25] C. Zhang, *Science China Physics, Mechanics and Astronomy* **53**, 2084 (2010).
- [26] S. Jadach, B. F. L. Ward, and Z. Was, *Phys. Rev. D* **63**, 113009 (2001).
- [27] K. A. Olive *et al.* (Particle Data Group), *Chin. Phys. C* **38**, 090001 (2014).
- [28] D. J. Lange, *Nucl. Instrum. Methods Phys. Res., Sect. A* **462**, 152 (2001); R. G. Ping, *Chin. Phys. C* **32**, 599 (2008).
- [29] J. C. Chen, G. S. Huang, X. R. Qi, D. H. Zhang, and Y. S. Zhu, *Phys. Rev. D* **62**, 034003 (2000).
- [30] Charge conjugation is always implied, unless specifically stated otherwise.
- [31] S. Agostinelli *et al.* (GEANT4 Collaboration), *Nucl. Instrum. Methods Phys. Res., Sect. A* **506**, 250 (2003).
- [32] N. N. Achasov and G. N. Shestakov, *Phys. Rev. D* **86**, 114013 (2012).
- [33] K. S. Cranmer, *Comput. Phys. Commun.* **136**, 198 (2001).
- [34] E. A. Jadach and V. S. Fadin, *Sov. J. Nucl. Phys.* **41**, 466 (1985).
- [35] S. Actis *et al.*, *Eur. Phys. J. C* **66**, 585 (2010); F. Jegerlehner *et al.*, *Nuovo Cimento C* **034S1**, 31 (2011).
- [36] M. Ablikim *et al.* (BESIII Collaboration), *Phys. Rev. D* **83**, 112005 (2011).
- [37] M. Ablikim *et al.* (BESIII Collaboration), *Phys. Rev. D* **81**, 052005 (2010).
- [38] K. S. Cranmer, *Comput. Phys. Commun.* **136**, 198 (2001).



TREASURES
@UT Dallas

School of Natural Sciences and Mathematics

*Observation of a Neutral Charmoniumlike State $Z_c(4025)^0$ in $e^+e^- \rightarrow (D^*D^*)^0\pi^0$*

©2015 American Physical Society

Citation:

Ablikim, M., M. N. Achasov, X. C. Ai, O. Albayrak, et al. 2015. "Observation of a Neutral Charmoniumlike State $Z_c(4025)^0$ in $e^+e^- \rightarrow (D^*D^*)^0\pi^0$." *Physical Review Letters* 115(18), doi:10.1103/PhysRevLett.115.182002

This document is being made freely available by the Eugene McDermott Library of The University of Texas at Dallas with permission of the copyright owner. All rights are reserved under United States copyright law unless specified otherwise.